A RIGOROUS ANALYSIS OF THE HIGHER ORDER MODES AND ATTENUATION OF STRIPLINE OF ARBITRARY DIMENSIONS

M.H.Burchett, S.R.Pennock, P.R. Shepherd,

School of Electronic and Electrical Engineering, University of Bath,
Claverton Down, Bath, Avon. BA2 7AY. United Kingdom

Abstract

This paper presents a rigorous and computationally efficient analysis for stripline of arbitrary dimensions based on the Transverse Resonance Diffraction technique. Calculated higher order mode cutoff frequencies show excellent agreement, and attenuation factor shows good agreement with measured values, and are more accurate than predictions from numerical or analytical techniques.

I. Introduction

Stripline is widely used as a structure for beam-forming networks in antenna systems where signal phase and amplitude must be closely controlled. A rigorous analysis is required to model these networks accurately with the desire to reduce the number of design iterations.

Conformal mapping analysis provides a closed form expression for the cutoff frequencies and attenuation factor of stripline. Cohn [1] first analysed stripline structures, recently the analysis has been simplified [2] to provide one form of the attenuation factor expression for a wide range of dimensions. Oliner [3] provided a conformal mapping expression for the higher order mode cutoff frequencies assuming an infinitely thin central conductor.

The conformal mapping expressions assume a quasi-static field and are only valid for a constrained range of dimensions. More accurate results can be obtained using numerical techniques.

Stripline has been analysed using finite difference [4] and finite element techniques [5]. These methods can be applied to structures with arbitrary dimensions but rely on the stripline being enclosed in a box. This gives rise to spurious modes when the higher order modes are computed. The disadvantage of the numerical techniques is the time taken to analyse straightforward stripline structures.

We present a rigorous and computationally efficient analysis for stripline based on the Transverse Resonance Diffraction (TRD) technique [6, 7]. The technique computes the field pattern around the uniform stripline, from which the impedance, power flow and power dissipation can be calculated.

II. Theory

The stripline structure is shown in Figure 1 and the problem is analysed in terms of a cascaded y parameter model for the TEM and TE modes. Relating the $\hat{z}$ directed magnetic field to the $\hat{x}$ directed electric field via Greens admittance operators, we find:

$$\begin{bmatrix} h^{II}_{zk1} \\ h^{II}_{zk2} \end{bmatrix} = \begin{bmatrix} y^{II}_{11} & y^{II}_{12} \\ y^{II}_{12} & y^{II}_{22} \end{bmatrix} \bullet \begin{bmatrix} e^{II}_{xk1} \\ e^{II}_{xk2} \end{bmatrix} \quad (1)$$

$$h^{I}_{zk1} = y^{I}_{1} \bullet e^{I}_{xk1} \quad (2)$$

$$h^{III}_{zk2} = y^{III}_{1} \bullet e^{III}_{xk2} \quad (3)$$

where $\bullet$ denotes convolution

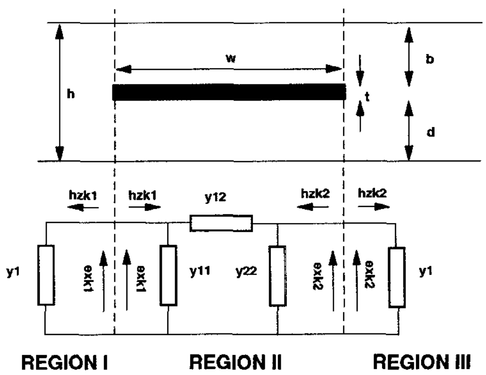

Figure 1: Uniform Stripline Structure and Equivalent y Parameter Circuit Model

Field continuity is enforced across the boundaries between Regions I and II, and Regions II and III. The e_{xk} fields are discretised using Gegenbauer polynomials to accurately model the $| r^{-\frac{1}{3}} |$ singularity present on the edge of the stripline. Galerkins method is applied giving the overall transverse resonance equation:

$$\begin{bmatrix} \underline{0} \\ \underline{0} \end{bmatrix} = \begin{bmatrix} [Y_1^I + Y_{11}^{II}] & [Y_{12}^{II}] \\ [Y_{12}^{II}] & [Y_1^{III} + Y_{22}^{II}] \end{bmatrix} \begin{bmatrix} \underline{X_p}^{I-II} \\ \underline{X_p}^{II-III} \end{bmatrix} \tag{4}$$

where:

$$\begin{aligned} [Y_{11}^{II}]_{pq} &= -C_{pq} \sum_n \left(\frac{\mathrm{ct}(kyn\frac{w}{2})}{kyn} + \frac{\mathrm{ct}(kym\frac{w}{2})}{kym} \right) \\ &\quad \bullet \mathcal{J}(p, n\pi)\, \mathcal{J}(q, n\pi) \end{aligned} \tag{5}$$

$$\begin{aligned} [Y_{12}^{II}]_{pq} &= C_{pq} \sum_n \left(\frac{\mathrm{csc}(kyn\frac{w}{2})}{kyn} + \frac{\mathrm{csc}(kym\frac{w}{2})}{kym} \right) \\ &\quad \bullet \mathcal{J}(p, n\pi)\, \mathcal{J}(q, n\pi) \end{aligned} \tag{6}$$

$$\begin{aligned} [Y_1^I]_{pq} &= C_{pq} \sum_n \frac{1}{j\, kyln} \mathcal{J}(p, k_n(b))\, \mathcal{J}(q, k_n(b)) \\ &+ C_{pq} \sum_n \frac{1}{j\, kylm} \mathcal{J}(p, k_n(d))\, \mathcal{J}(q, k_n(d)) \end{aligned} \tag{7}$$

$$[Y_1^{III}] = [Y_1^I] \tag{8}$$

$$[Y_{22}^{II}] = [Y_{11}^{II}] \tag{9}$$

$$[Y_{21}^{II}] = [Y_{12}^{II}] \tag{10}$$

where :

$$\begin{aligned} \mathcal{J}(m, \alpha) &= J_{2m+\frac{1}{6}}(\alpha) \\ k_m(a) &= \frac{m\pi a}{2(a + \frac{t}{2})} \\ C_{pq} &= (-1)^{p+q} \frac{-k_t^2 \pi}{2\omega\mu_0} \bullet \\ &\left[\frac{\Gamma(2p + \frac{1}{3})\Gamma(2q + \frac{1}{3})}{(2p)!\,(2q)!} \right]^{\frac{1}{2}} \left[\left(2p + \frac{1}{6}\right) \left(2q + \frac{1}{6}\right) \right]^{\frac{1}{2}} \end{aligned}$$

Solving equation 4 determines the cutoff wavenumbers and basis amplitude terms, and so the fields of the structure can be calculated.

The attenuation factor is found from:

$$\alpha = \left(\frac{Power\ Dissipated\ in\ Structure}{2 \times Power\ Flow\ in\ Structure} \right) \tag{11}$$

$$= \frac{P_{dis}}{2 \times P_{flow}} \tag{12}$$

where

$$P_{dis} = \frac{1}{2} R_s \int_{CrossSection} \hat{n} \wedge \underline{H}\ \underline{da} \tag{13}$$

$$P_{flow} = \int_{CrossSection} \underline{E} \wedge \underline{H}\ \underline{da} \tag{14}$$

The results presented in this paper are in terms of the normalised attenuation factor, α_n, where

$$\alpha_n = 20\ \log_{10} e \left(\frac{h}{R_s} \right) \alpha \quad dBm^{-1} \tag{15}$$

This normalisation removes the effect of frequency and the surface resistance R_s of the strip and ground planes.

III. Results and Discussion

Convergence of the Method

Results are presented in Tables 1 and 2 showing the convergence of the cutoff frequency for the first and second higher order modes. The results show that only two basis functions and five field expansion terms are required to compute the values to within one percent.

N	No. of Basis Functions, P				
	1	2	3	4	5
5	7.029	7.040	7.057	7.080	7.091
10	6.995	7.000	7.005	7.012	7.021
15	6.986	6.989	6.992	6.996	7.000
25	6.980	6.982	6.983	6.985	6.986
50	6.975	6.977	6.978	6.978	6.979
75	6.973	6.975	6.976	6.976	6.977
100	6.973	6.974	6.975	6.976	6.976
200	6.972	6.974	6.974	6.975	6.975

Table 1: Table of First Higher Order Mode Convergence with the Number of Field Expansion Terms, N, and the Number of Basis Functions, P.

N	No. of Basis Functions, P				
	1	2	3	4	5
5	11.732	11.796	11.797	11.799	11.800
10	11.732	11.793	11.794	11.794	11.795
15	11.732	11.792	11.793	11.793	11.794
25	11.732	11.792	11.792	11.792	11.792
50	11.731	11.791	11.792	11.792	11.792
75	11.731	11.791	11.791	11.792	11.792
100	11.731	11.791	11.791	11.791	11.791
200	11.731	11.791	11.791	11.791	11.791

Table 2: Table of Second Higher Order Mode Convergence with the Number of Field Expansion Terms, N, and the Number of Basis Functions, P.

Higher Order Mode Cutoff Frequencies

The variation in cutoff frequency with strip width was compared to measurement, to Hewlett Packard's Finite Element

High Frequency Structure Simulator (HFSS) software and to Oliner's paper [3]. The measurements were taken with an HP8510B using a lightly coupled probe resonator technique [7]. The results are compared in Figure 2 and Figure 3 showing the percentage error between calculation and measurement. The agreement between measured and TRD results is within two percent and typically within one percent. The rigorous analysis and precise measurement of test fixture dimensions ensures that the agreement is limited by the measurement accuracy. Oliner's analysis provides a consistent overestimate. The errors can be attributed to the assumptions of a zero thickness central conductor and limitations of the conformal mapping technique. The HFSS computes the first higher order box mode and stripline mode. The box mode tends towards zero as the strip width increases. The error for the stripline mode is typically within five percent with agreement improving as the strip width increases. The HFSS computes upper and lower limits for the second higher order mode with an average error of between seven percent and one percent. The computation of upper and lower limits was also observed with the TEM propagation constant.

Normalised Attenuation Factor, α_n	
Cohn	0.06484
TRD	0.05879
HFSS(Lower Limit)	0.06522
HFSS(Upper Limit)	0.06809

Table 3: Table of Normalised Attenuation Factor for a symmetrical strip of width 14mm and thickness 1.6mm

Attenuation Factor

The attenuation factor results from the TRD analysis were compared with Cohns analysis [1] and the HFSS software. The values of normalised attenuation factor are tabulated in Table 3 for a nominally 50Ω stripline. The TRD value differs by ten percent from Cohn's value and by fourteen percent from the HFSS values.

The Q factor was measured using the lightly coupled probe resonator technique. The normalised attenuation factor was calculated from equation 16. The effect of surface roughness is calculated from a formula given in [8].

$$\alpha_{Neff} = \frac{[h\sqrt{\pi\epsilon_0}][20\log_{10} e]}{Q_m\left[1+\frac{2}{\pi}\tan^{-1}\left(1.4\left(\frac{\Delta}{\delta_s}\right)^2\right)\right]}\sqrt{\frac{f}{\rho}}\left(\frac{\beta}{k_0}\right)^{-1} \quad (16)$$

where Δ is the rms surface roughness
δ_s is the skin depth
Q_m is the measured Q factor

The average measured and computed attenuation factor values are plotted in Figure 4. The error bars mark the standard deviation of the measured values.

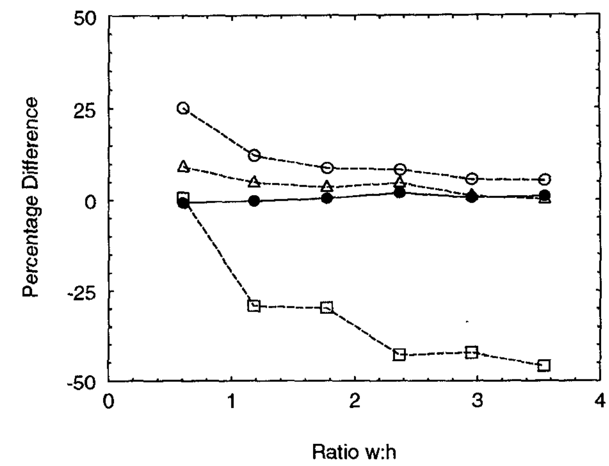

Figure 2: Percentage Variation between Measured Cutoff Frequencies and Computed Cutoff Frequencies for the First Higher Order Mode Calculated by HFSS (Stripline Mode)[△] and (Box Mode)[□]; Oliner's Analysis [o] and TRD Analysis [•] for h=11.850mm, t=1.620mm, b=4.965mm and d=5.265mm.

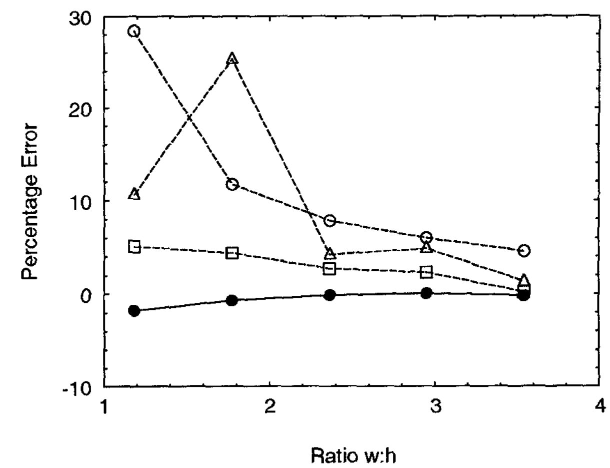

Figure 3: Percentage Variation between Measured Cutoff Frequencies and Computed Cutoff Frequencies for the First Higher Order Mode Calculated by HFSS (Upper Limit)[△] and (Lower Limit)[□]; Oliner's Analysis [o] and TRD Analysis[•] for h=11.850mm, t=1.620mm, b=4.965mm and d=5.265mm.

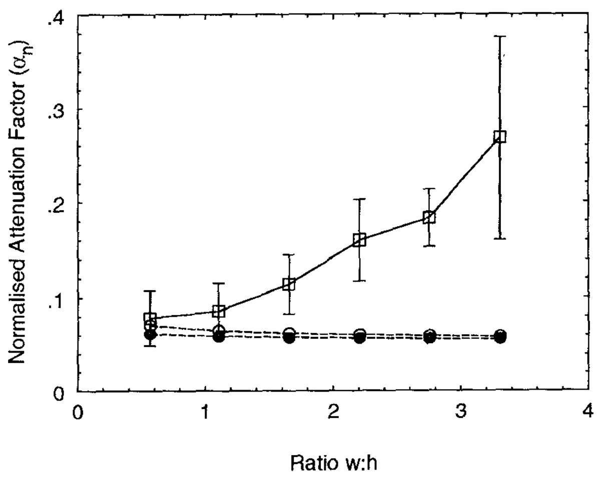

Figure 4: Measured Values (——) [$\rho = 90n\Omega m$] and Computed Values (- - -) of Normalised Attenuation Factor Calculated by Cohn's Analysis [o] and TRD Analysis [•] for h=11.850mm, t=1.620mm, b=4.965mm and d=5.265mm

The error between Cohn's and the TRD values ranges from five to fourteen percent. The measured values show reasonable agreement for relatively narrow strip widths, but a considerable error for wider strips.

The error for wide strips is due to the probe being unable to efficiently couple to the cavity modes. Progressively more power is also lost due to radiation out of the sides of the test fixture as the strip width increases. The theoretical calculations do not take this into account.

IV. Conclusions

The Transverse Resonance Diffraction (TRD) results presented have been shown to be in excellent agreement with measured values and offer improved accuracy over numerical techniques. However the time required to compute the data is considerably less, and the algorithm can be programmed on a desktop computer.

The characteristic impedance of stripline can also be easily computed, and the theory extended to analyse any number of coupled striplines of arbitrary dimensions. These aspects of the analysis are currently in progress.

V. Acknowledgements

This work was supported by an SERC CASE Studentship Award in conjunction with Siemens Plessey Systems Limited, Isle of Wight, United Kingdom.

References

[1] Cohn S.B. Problems in strip transmission lines. *IEEE Transactions on Microwave Theory and Techniques*, MTT-3:119–126, March 1955.

[2] Rawal S. and Jackson D.R. An exact TEM calculation of loss in a stripline of arbitrary dimensions. *IEEE Transactions on Microwave Theory and Techniques*, MTT-39:694–699, April 1991.

[3] Oliner A.A. Equivalent circuits for discontinuities in balanced strip transmission lines. *IEEE Transactions on Microwave Theory and Techniques*, MTT-3:134–143, March 1955.

[4] Schneider M.V. Computation of impedance and attenuation of TEM lines by finite difference methods. *IEEE Transactions on Microwave Theory and Techniques*, MTT-13:793–800, November 1965.

[5] Pantic Z. and Mittra R. Quasi-TEM analysis of microwave transmission lines by the finite element method. *IEEE Transactions on Microwave Theory and Techniques*, MTT-34:1096–1103, November 1986.

[6] Rozzi T.E. and De. Leo R. Rigorous analysis of the GTEM cell. *IEEE Transactions on Microwave Theory and Techniques*, MTT-39:488–499, March 1991.

[7] Izzat N. Pennock S.R. and Rozzi T.E. Very wideband operation of twin layer inset dielectric guide. *IEEE Transactions on Microwave Theory and Techniques*, MTT-40:1910–1917, October 1992.

[8] Edwards T.C. *Foundations for Microstrip Circuit Design.* Wiley, 1992.